A&A manuscript no.
(will be inserted by hand later)

Your thesaurus codes are:
07 (08.01.1; 08.01.3; 08.06.3; 08.08.1; 08.13.2; 08.23.2)

ASTRONOMY
AND
ASTROPHYSICS
27.1.1995

Spectral analyses of the Galactic Wolf-Rayet stars: hydrogen-helium abundances and improved stellar parameters for the WN class⋆

W.-R. Hamann⋆⋆, L. Koesterke⋆⋆, and U. Wessolowski⋆⋆

Institut für Theoretische Physik und Sternwarte der Universität, Olshausenstraße 40, D-24118 Kiel, Germany
E-mail (W.-R.H.): pas81@rz.uni-kiel.d400.de

Received date; accepted date

Abstract. Almost all known Galactic single WN stars have been analyzed applying non-LTE models for spherically expanding atmospheres. While in a previous study we performed "coarse" spectral analyses based essentially on helium-line *equivalent widths* compared to a grid of models, we now present improved results from 25 detailed "fine" analyses, i.e. from fitting the *line profiles* with individual model calculations. The non-LTE models applied now account for a helium-hydrogen composition, and corresponding abundances are determined for each star.

53% of the studied Galactic WN stars (33 out of 62) are hydrogen-free, populating a luminosity range from $10^{4.6}$ to $10^{5.7}\,L_\odot$. The occurrence of hydrogen is restricted to those WN stars with lowest stellar temperatures (30 ... 35 kK, with few exceptions), comprising most stars of late subtype (WNL) and part of the weak-lined early-type WN stars (WNE-w). But all WN stars are definitely hydrogen-deficient, compared to the solar value. Most WN stars showing hydrogen exhibit mass fractions $\beta_{\rm H}$ between 10% and 30%. They cover the whole luminosity range of the the hydrogen-free WN stars, but extend also to higher values: a group of ten WNL stars with hydrogen is brighter than $10^{5.7}\,L_\odot$, i.e. brighter than any hydrogen-free WN star. Only three WN stars are found with hydrogen mass fractions as small as $\approx$ 5%. A small group of four WN7 stars with high luminosities ($> 10^{5.6}\,L_\odot$) has outstandingly high hydrogen mass fractions (40 ... 53%).

The gradual switching from the high mass-loss rates of the hydrogen-free WN stars to the much lower mass-loss rates of typical OB stars is found to be correlated with the hydrogen abundance.

Key words: Stars: abundances – Stars: atmospheres – Stars: fundamental parameters – Hertzsprung-Russell (HR) diagram – Stars: mass loss – Stars: Wolf-Rayet

1. Introduction

The quantitative analysis of Wolf-Rayet (WR) spectra became possible in the last decade with the development of model calculations for non-LTE radiation transfer in spherically expanding stellar atmospheres, which was achieved independently by Hillier (see e.g. 1990 and references therein) and by our group. By means of a new solution method ("iteration with approximate lambda operators") we could present a grid of models for pure-helium atmospheres (Wessolowski et al. 1988). These models were tested first in a few detailed analyses (Hamann et al. 1988, Schmutz et al. 1988) and then applied for coarse analyses of greater samples (30 Galactic WR stars: Schmutz et al. 1989; 19 stars in the Large Magellanic Cloud: Koesterke et al. 1991). In a comprehensive study (Hamann et al. 1993, in the following referred to as Paper I) we performed "coarse" analyses of the vast majority of the Galactic WN stars (remember that the WR stars are divided into a nitrogen – WN – and a carbon – WC – spectral sequence). Based on the grid of pure-helium models, the stellar parameters were determined from the measured equivalent widths of strategic helium lines. Moreover, the presence or absence of hydrogen in the WR atmospheres was assessed qualitatively by inspection of the H I-Balmer/He II-Pickering decrement.

The first quantitative estimates of hydrogen abundances in WN stars (Castor & Van Blerkom 1970; Smith 1973; Conti et al. 1983) were based on a highly simplified theoretical approach. In the present work we now determine the hydrogen abundances quantitatively from detailed model calculations and profile fits of the helium und hydrogen lines. As a by-product of these "fine" analyses, improved parameters are derived for many WN

Send offprint requests to: W.-R. Hamann

⋆ Based, in part, on observations collected at the European Southern Observatory (ESO), La Silla, Chile

⋆⋆ Visiting astronomers, German-Spanish Astronomical Center, Calar Alto, operated by the Max-Planck-Institut für Astronomie, Heidelberg, jointly with the Spanish National Commission for Astronomy

stars. In addition to Paper I, new observations are introduced which allow to analyze six further WN stars. In the representation of the results we include WN stars of earliest subtype which can not be analyzed from their helium spectrum alone because of the absence of He I lines, but which are presently analyzed (Wessolowski et al., in preparation) by means of their nitrogen lines.

The applied model atmospheres are characterized in the following section (Sect. 2). Subsequently the observational data are introduced (Sect. 3), while the methods of our spectral analyses are described in Sect. 4. The results are comprehensively compiled in Sect. 5.

2. The models

2.1. Basic assumptions and methods

The model calculations are of similar kind as described in previous papers (Hamann & Schmutz 1987, Wessolowski et al. 1988), and the reader is referred to these papers for more details and references. Only the basic assumptions and definitions are briefly repeated here.

A "standard" WR atmosphere is assumed to be expanding in a spherically-symmetric, homogeneous and stationary flow. With a given mass-loss rate $\dot{M}$, the density stratification and the velocity field $v(r)$ are related via the equation of continuity.

The velocity field is pre-specified from plausible ad-hoc assumptions. For the supersonic part we adopt the usual *β-law* (cf., e.g., Paper I, Eq. 1) with the terminal velocity v_∞ being a free parameter. The exponent β is set to unity throughout this work. In the subsonic region the velocity field is defined such that a hydrostatic density stratification is approached.

Using the *β-law* for WR winds is justified only from the empirical experience that it yields reasonable line fits. However, from hydrodynamic modelling Springmann (1994) expects that the velocity law of WR winds, if driven by multiple line scattering radiation pressure, should approach the form $\sqrt{\ln(r/R_*)}$. Taking this literally, we performed a couple of test calculations. After suitable adjustment of the velocity gradient (note that Springmann's law does not approach any terminal velocity) we obtained an almost identical fit of the helium und hydrogen lines, compared to the calculations with the *β-law*. The parameters for the best-fitting models differed only marginally between both cases. Hence these tests confirm once more our experience that the choice of the velocity-law does not have significant influence on the derived stellar parameters and atmospheric abundances.

The "stellar radius" R_*, which is the inner boundary of our model atmosphere, corresponds per definition to a Rosseland optical depth of 20. In the whole relevant range of model parameters, the expansion velocity at R_* is still subsonic. Thus, R_* can be regarded as the radius of the hydrostatic stellar core.

The "stellar temperature" T_* is defined by the luminosity L and the stellar radius R_* via the Stefan-Boltzmann law, i.e. T_* denotes the effective temperature referring to the radius R_*. Different definitions of the reference radius and, correspondingly, of the "effective temperature" will be considered as well (cf. Sect. 5.2).

The temperature stratification is calculated in advance from the assumption of radiative equilibrium, which is evaluated in the grey, LTE approximation. The radial decrease of the electron temperature is artificially stopped at a minimum value of 10 kK. The resulting temperature stratification is in sufficient agreement with detailed non-grey non-LTE models accounting for nitrogen (Hamann & Wessolowski 1990).

Only Doppler broadening is accounted for in the profile function of the line absorption coefficient. The Doppler-velocity $v_{\rm D}$ reflects random motion on small scales and is generally set to 100 km s^{-1}. A "microturbulence" of that order-of-magnitude reproduces best the detailed shape of the observed line profiles. Its precise value does not have significant influence on the results of our spectral analyses.

The line radiation transfer in the spherically expanding geometry is formulated in the comoving-frame of reference (CMF). Continuum formation is treated with the moment equations and variable Eddington factors. The equations of statistical equilibrium account for all relevant radiative and collisional transition rates. The consistent solution of both sets of equations, radiation transfer and statistical equilibrium, is achieved by "iteration with approximate lambda operators" (cf. Hamann 1985, 1986, 1987; Koesterke et al. 1992). The obtained non-LTE population numbers enter the subsequent Formal Integration of the transfer equation in the observer's frame which is performed by straightforward integration along each ray.

Note that the overlap of blending lines is treated correctly at both stages, in the CMF radiation transfer for calculating the population numbers and in the formal integration in the observer's frame for the emergent profiles, as described in Hamann et al. (1991).

The model atmosphere is assumed to consist of helium and hydrogen, using the hydrogen mass fraction $\beta_{\rm H}$ as parameter. The helium model atom accounts for 17 bound levels of He I 16 levels of He II and He III. The hydrogen atom is described by ten bound levels of H I and H II.

In addition to Paper I, frequency redistribution of line photons by electron scattering is now accounted for as described by Hamann et al. (1992) in those model calculations applied for the profile fitting ("fine" analyses).

Summarizing, any particular model is specified by its basic parameters R_*, T_*, $\dot{M}$, v_∞ and $\beta_{\rm H}$.

Synthetic spectra from Wolf-Rayet model atmospheres of different mass-loss rates, stellar radii and terminal wind velocities yield the same emission line equivalent widths, if they agree in their "transformed radius" $R_{\rm t}$ (and, of course, the other relevant parameters), where $R_{\rm t}$ is defined by

$$R_{\rm t} = R_* \left[\frac{v_\infty}{2500\,{\rm km\,s^{-1}}} \Big/ \frac{\dot{M}}{10^{-4}\,M_\odot\ {\rm yr^{-1}}} \right]^{2/3} . \qquad (1)$$

(cf. also Paper I). Thus $R_{\rm t}$ is a basic parameter of expanding atmospheres and has the advantage that its determination is

independent from any adopted distance or absolute brightness of the star. In this respect, R_t plays a similar role for expanding atmospheres as $\log g$ in the static case. Due to the homology of the models with same R_t, the intrinsic color index $(b-v)_0$ is also derived from the line fit before any distance-dependent quantities are introduced.

3. The observations

Most analyses presented here are based on spectra obtained 1991 at the "Deutsch-Spanisches Astronomisches Zentrum (DSAZ)", Calar Alto, Spain, and 1992 at the European Southern Observatory (ESO), La Silla, Chile (for details see Paper I).

These older data are augmented by new spectroscopic observations of some northern WN stars collected by two of us (W.-R. H. and U. W.) between July 3 and 12, 1993, at the DSAZ. We used the 2.2m-telescope with the Boller & Chivens Cassegrain spectrograph and a coated CCD (TEK). Three exposures per star were made with different grating angles, covering the wide spectral range from 3430 to 7200 Å with a spectral resolution of about 3600.

The spectra were extracted from the images with the MIDAS software. After division by a fit to the continuum of a comparison star, the continuum was defined in each of the three parts of the spectrum by fitting a low-order polynomial.

These new observations are applied for the "fine analyses" of WR 105 and the six newly analyzed stars compiled in Table 1.

4. The analyses

4.1. The Galactic WN stars: identification and classification

An update of the Sixth Galactic WR Catalog (van der Hucht et al. 1981) has been given by van der Hucht et al. (1988). It comprises 71 stars of WN subtypes (another 13 stars which joined the WN class more recently, cf. van der Hucht 1992, are not yet included in our program), when leaving aside those 14 stars which are classified as binaries with massive companions because of composite spectra (cf. Table 1 in Paper I). However, we include those stars which are said to be single-lined spectroscopic binaries (SB1). These stars may indeed have a less luminous companion (which would not contaminate the spectrum and thus would not influence the result of our analysis), or the observed radial velocity variations might be due to radial pulsations or to instationary mass-loss.

Throughout this paper, the WR stars are identified by their number in these catalogs. The spectral subtype classification is also quoted from van der Hucht et al. (1988). (Only for one star, WR 91, we have changed the classification from WN7 to WN6-s, cf. Paper I). The WN subtype number essentially reflects the line strength ratios between different ionization stages of nitrogen. Remember that the subtypes WN2 to WN6 are called "early" (WNE), while from WN7 they are termed "late" (WNL). An additional "a" (abbreviating "+abs") is attributed according to van der Hucht et al. (1988) to those spectra showing not only emission, but also "absorption lines which have not been shown to be due to a companion". (Absorption features of that kind can be reproduced in principle by our single-star models.) A "+c" added to the spectral type denotes putative single-lined spectroscopic binaries. For WNE stars we append "-w" or "-s" to the classification, indicating whether the emission lines are weak or strong, respectively. The criterion is whether the equivalent width of the He II line at 5412 Å is smaller or larger than 37 Å. We have slightly diminished this limit compared to previous papers (40 Å), because it seems to be more adequate to put WR 91 with W_λ(He II 5412) = 38 Å and WR 149 (39 Å) into the "strong line" subgroup, as will become obvious below.

4.2. Six newly analyzed WN stars

In Paper I we had studied 56 Galactic WN stars. Meanwhile we obtained observations of six additional stars, which are analyzed here in order to complete our sample further. The stars and the strategic helium line equivalent widths are given in Table 1. When measuring the equivalent widths we disregard any weak, extended (electron-scattering?) wings if present. The interstellar Na I absorption blending He I 5876 was removed "by hand". The given equivalent widths are "net" values (positive for emission), i.e. contribution from (P-Cygni) absorption features are subtracted.

WR 157 was not resolved in our observation (nor, presumably, in the IR observation by Vreux et al. 1990 quoted in Table 1) from its visual companion 1" apart, which is 0.2 mag brighter and of type B0III (Wilson 1940). Assuming that the continua of both stars are parallel, we scaled the observed equivalent widths with a factor 2.2.

Table 1. Measured equivalent widths of strategic helium lines for six Galactic WN stars augmenting Table 2 in Paper I

		W_λ [Å]		
WR	Type	He II 5412	He I 5876	He I 10830
116	WN8	3	45	-
130	WN8	5	14	-
147	WN7	4	27	-
149	WN6-s	39	10	-
155	WN7 +c	7	4	68[a]
157[b]	WN4.5-w	18	4	60[a]

[a] Average of the values from Kuhi (1968) and from Vreux et al. (1990)

[b] Observed values have been scaled with a factor 2.2 to correct for the unresolved visual companion (see text)

4.3. "Fine analyses" of 25 WN stars

In order to determine the hydrogen abundances quantitatively, individual model calculations and profile fits are performed for 25 Galactic WN stars. The sample comprises all WN stars for

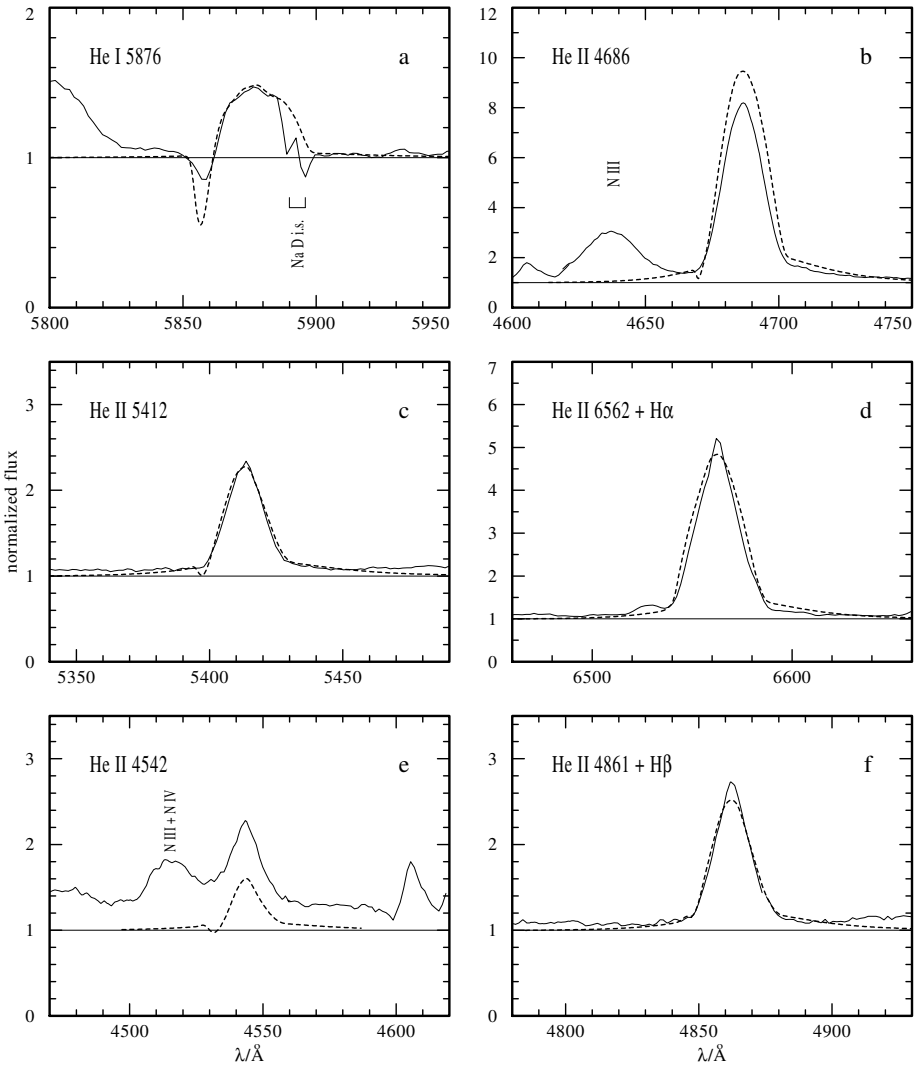

Fig. 1. Fit of the helium and hydrogen line profiles for WR 35 as an example. The observed spectrum (obtained with the ESO 3.6m telescope and EFOSC in echelle mode) is compared to the model (dashed) with suitably adjusted parameters (cf. Table 3).

which the presence of hydrogen was not ruled out from the qualitative inspection of the H I-Balmer–He II-Pickering decrement, but we leave out a couple of stars for which the hydrogen abundance was already determined with similar methods as used here (Hamann et al. 1991, Crowther et al. 1994a,b and in preparation). The sample also includes the six WN stars newly analyzed here (cf. preceding subsection).

The lines He II 5412 and He I 5876 (and He I 10830 if available) are of strategic importance for the analyses (cf. Schmutz et al. 1989). He II 4686 is less appropriate, as the continuum is difficult to define in its neighborhood, and moreover this line often results a bit too strong from the models for some unknown reason.

The determination of the hydrogen fraction in the helium-dominated WN atmospheres is hampered by the fact that all spectral lines of hydrogen coincide with lines of ionized helium, the principle quantum numbers of the involved He II levels being twice of the corresponding H I levels. Those He II lines with odd principle quantum number(s) remain unblended. Thus we must first achieve a good fit to the unblended He II lines, before the *excess* contribution from hydrogen to the (generally strong) blended He II lines can be identified.

The visual spectrum thus offers the He II Pickering series (4-n) from n=6 (6562 Å, Hα) to n=11 (4200 Å). He II 4101 (n=12, Hδ) is not useful because it is blended with N III lines. Higher series members are generally too weak, and the observed spectra are often too noisy in their bluemost part. Hence the hydrogen abundance is essentially derived from Hα and Hβ in comparison with He II 5412.

Starting with the stellar parameters from the "coarse analysis" and a first guess on the hydrogen abundance, the parameters are varied until the theoretical profiles fit best to the observed helium and hydrogen lines. An example for the achieved agreement is shown in Fig. 1. Generally the final parameters do not differ much from the "coarse analyses" results. The only exception is WR 152, for which the detailed fit to the marginal He I

Table 2. Distance modulus, color index and absolute visual magnitude for the Galactic single WN stars newly analyzed here (augmenting Table 4 in Paper I). If the star is assigned to an open cluster or association (entry given in the third column), the absolute visual magnitude M_v follows from the given distance modulus DM. Otherwise, M_v is assumed from an empirical calibration considering subtype, temperature and transformed radius of the star (see Paper I), and DM finally results.

WR	Type	Cluster/ Assoc.		DM [mag]	m_v [mag]	$b-v$ [mag]	$(b-v)_0$ [mag]	E_{b-v} [mag]	A_v [mag]	M_v [mag]
(1)	(2)	(3)	(4)	(5)	(6)	(7)	(8)	(9)	(10)	(11)
3^{N}	WN3a-w +c	-		12.4	10.70	-0.06	-0.36	0.30	1.23	-2.9
46^{N}	WN3pec-w	-		12.5	10.96	0.00	-0.34	0.34	1.39	-2.9
116	WN8	-		12.1	13.38	1.41	-0.28	1.69	6.93	-5.7
130	WN8	-		13.3	12.60	1.18	-0.28	1.46	5.99	-6.7
136^{a}	WN6-s +c	Cyg OB1	:	11.3	7.65	0.23	-0.12	0.35	1.44	-5.1
147	WN7	-		10.6	14.89	2.15	-0.28	2.43	9.96	-5.7
149	WN6-s	-		14.9	14.70	1.20	-0.20	1.40	5.74	-5.9
155	WN7 +c^{b}	Cep OB1	:	12.7	8.75	0.28	-0.29	0.57	2.34	-6.3
157	WN4.5-w	Ma 50	+	12.8	9.91	0.46	-0.28	0.74	3.03	-5.9

Column 4 indicates whether the quoted cluster/association membership is "definite" (+) or "probable" (:) according to Lundström & Stenholm (1984).

^{N} Intrinsic color index from analysis of the nitrogen spectrum (preliminary result from Wessolowski et al., in preparation)

^{a} The entry for WR 136 is included here as an erratum to Paper I, because we repeated there an earlier misprint (from Lundström & Stenholm 1984) assigning this star to Cyg OB3 and therefore arrived at a slightly wrong absolute magnitude.

^{b} WR 155 rejected as WN7 + O system by Leung et al. (1983). Its membership to Cep OB1 was erroneously omitted in Paper I.

line at 10830 Å (using the observation by Howarth & Schmutz 1992) now yields a significantly higher effective temperature and luminosity.

4.4. The WN stars of earliest subtype

In three spectra (WR 2, WR 3, WR 46) all He I lines are weaker than the detection limit. Hence it is not possible to analyze these stars with the technique of the present paper which essentially relies on the He II/He I line ratios. But, due to the progress in the model calculations, we can analyze these stars now using their nitrogen lines (Wessolowski et al., in preparation). However, results from this new method which is essentially based on the N V/N IV line ratios are not fully consistent with the results from the helium analyses applied else. Tests with WR 152, for which both methods can be used, revealed that considerably higher stellar temperatures T_* are derived from the N V/N IV line ratio than from He II/He I (75 kK and 49 kK, respectively; cf. also Crowther 1993). The discussion of these problems is beyond the scope of the present paper, but they should be kept in mind when the preliminary parameters for WR 3 and WR 46 are included in the following figures and tables. The analysis of WR 2, which seems to be the hottest Galactic WN star, is still in progress and no results can be given yet.

4.5. Distance and absolute visual magnitude

Table 2 gives the photometric data for the newly analyzed stars. When Lundström & Stenholm (1984) assigned the star to an open cluster or association, this is indicated in the third column together with their rating of the membership reliability (Column 4, see legend). For those stars for which Column 3 displays an cluster/association entry, Column 5 gives the corresponding distance modulus (DM) (also taken from Lundström & Stenholm 1984). Columns 6 and 7 give the observed photometric v magnitude and the color index $b-v$ in the narrow-band system of Smith (1968), as compiled by van der Hucht et al. (1988). We identify these colors with the theoretical continuum, and do not try to correct them for a possible "line contamination". Column 8 gives the intrinsic color index $(b-v)_0$ which follows from the models. The comparison of Columns 7 and 8 yields the color excess E_{b-v} (Column 9). The interstellar extinction in the v band (Column 10) is obtained from $A_v = 4.1\, E_{b-v}$ (Lundström & Stenholm 1984). When the distance modulus DM is known from its association membership, its absolute magnitude M_v (Column 11) follows from $M_v = m_v - DM - A_v$. For the other stars of Table 2, the M_v calibration from Paper I is adopted and DM follows.

5. Results

Table 3 contains all 71 single Galactic WN stars identified by their WR number (Column 1). An asterisk marks stars which we have "fine-analyzed"; otherwise the parameters are repeated from Paper I. An "N" superscript refers to preliminary results from analyses of the nitrogen lines (cf. Sect. 4.4). Spectral subtypes (cf. Sect. 4.1) are given in Column 2. Stars with known distance (cluster or association membership) are marked in Column 3 (cf. Sect. 4.5).

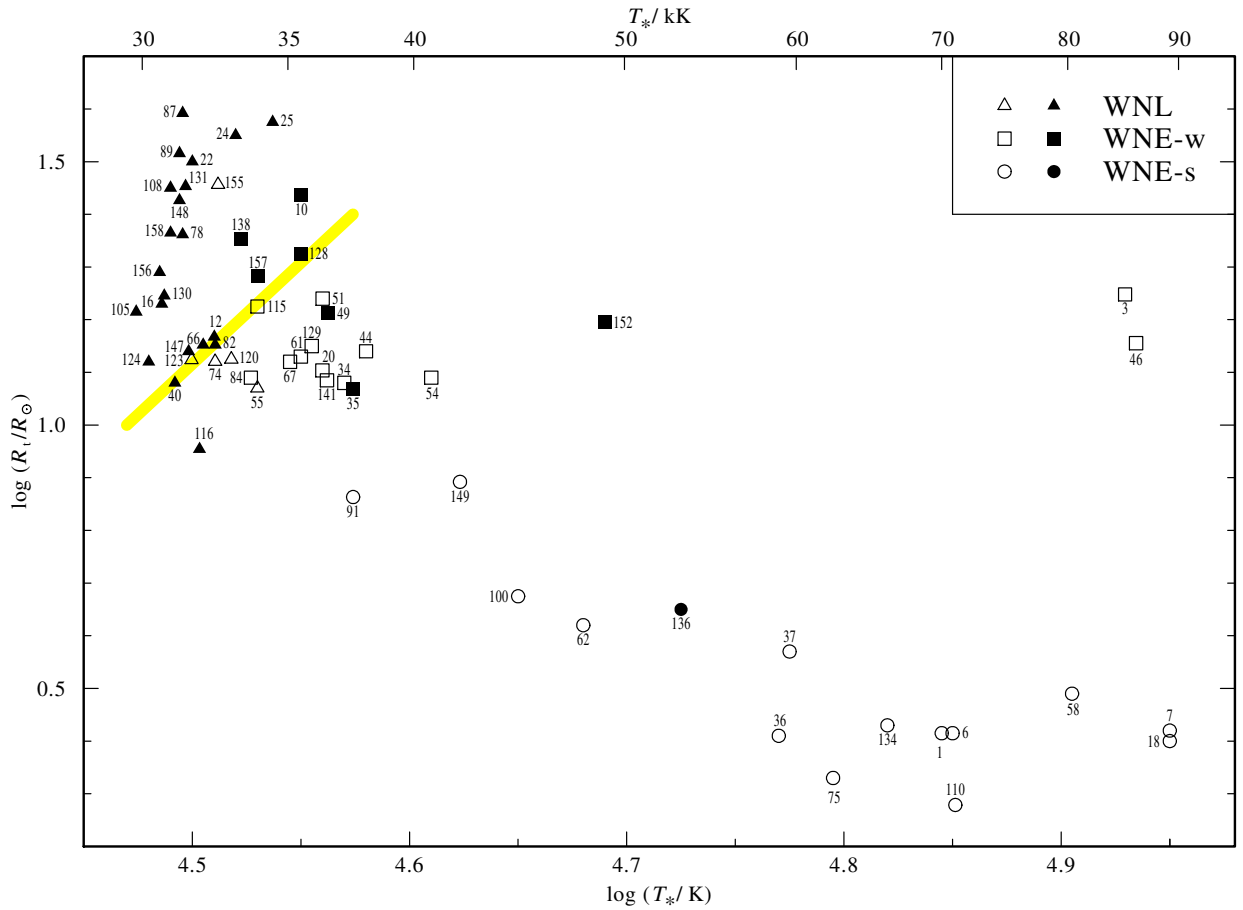

Fig. 2. Positions of the analyzed WN stars in the log T_*-log R_t-plane. The spectroscopic subclasses are distinguished by different symbol shapes (see inset). Filled symbols denote stars with hydrogen being detected in their spectra, while open symbols refer to stars without hydrogen. The borderline (shaded) between the hydrogen and the no-hydrogen regime does not fully coincide with the subclass domains.

5.1. Temperature and transformed radius

The stellar temperature and the "transformed radius" (cf. Eq. 1) of the Galactic WN stars are given in Table 3, Columns 4 and 6. Note that these parameters follow from the spectroscopic analyses alone, not involving yet any assumptions on the distance or absolute magnitudes of the stars. The positions of the program stars in the log T_*-log R_t-plane are shown in Fig. 2. The WNL stars have the largest transformed radii ($R_t > 10\,R_\odot$) and smallest stellar temperatures ($T_* \approx 30 ... 35$ kK). The WNE-w stars cover a similar range of R_t as the WNL stars (with a tendency to smaller values) but are slightly hotter (≈35 ... 40 kK). However, the WN2-w and WN3-w stars (WR 3, 46 and 152) are considerably hotter and form a separate group. (This is not only an artificial effect caused by the different methods of the analyses as discussed in Sect. 4.4.) The WNE-s stars populate an extended strip from 40 to 90 kK with small transformed radii, which decrease with temperature from 8 to 2 $R_\odot$. The clear separation and relative arrangement of these different groups in the log T_*-log R_t-plane is very puzzling. The division of the WNE stars into those with weak (WNE-w) and strong (WNE-s) lines obviously makes sense, as it discriminates between groups with rather different parameters.

In anticipation from Sect. 5.6 the presence or absence of hydrogen is also encoded in Fig. 2 by filled and open symbols, respectively. The conclusion from Paper I is confirmed by the more complete and partly corrected data shown here: WN stars with hydrogen and without hydrogen populate different domains in the log T_*-log R_t-plane. The borderline does not coincide exactly with the subclasses, but – roughly spoken – most WNL stars show hydrogen, while most WNE-w stars and almost all WNE-s stars are hydrogen-free. A few stars are violating the borderline in Fig. 2: WR 155 (WN7+c) lies in the hydrogen region but does not show hydrogen, while vice versa WR 116 (WN8) lies below the borderline although hydrogen is detected. Among the WNE-w there are three stars (WR 35: WN6-w, WR 49: WN5-w, and WR 152: WN3-w) with hydrogen lying at the "wrong" side. Most strikingly, WR 136 often considered as the WN6 prototype (!) is the only WNE-s star in which hydrogen is detected.

5.2. Photospheric radius and effective temperature

Column 7 gives the "photospheric radius" $R_{2/3}$ (in units of R_*) defined by a radial Rosseland optical depth of 2/3, while $T_{2/3}$ (Column 5) is the effective temperature referring to that radius (remember that T_* is the effective temperature referring to the radius of the hydrostatic core, R_*). While for the WNL and WNE-w stars $R_{2/3}/R_*$ is not much larger than unity, the atmospheres of the WNE-s stars are "extended" in the sense that the continuum is formed in layers which are already rapidly expanding, i.e. at radii $R_{2/3}$ significantly larger than the radius of the hydrostatic core. Consequently, for the WNE-s stars the temperature $T_{2/3}$ is significantly lower than T_*, while for the other stars the effective temperature is not sensitive to the choice of the reference radius.

Note that in principle the values of R_* and T_* depend on the adopted subphotospheric velocity law, which is not observationally constrained and for which no theory exists yet (see the corresponding discussion by Hamann 1994). Thus $T_{2/3}$ and $R_{2/3}$ might be considered as the original empirical parameters which are determined by our spectral analyses.

Column 5 reveals, as a very puzzling fact, that the values of $T_{2/3}$ scatter only over a rather narrow range. Only the WN2-w and WN3-w stars show outstandingly high values of $T_{2/3}$.

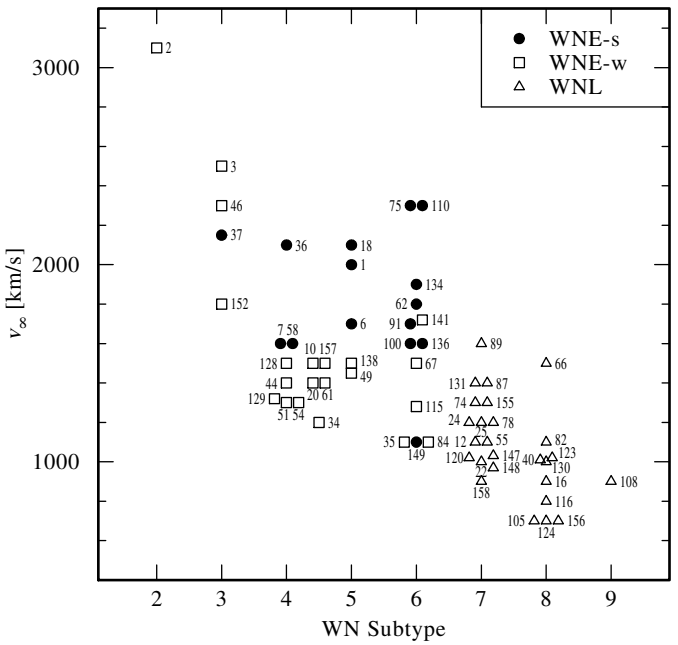

Fig. 3. Terminal velocities versus spectral subtype (labels: WR number). Different symbols refer to the spectral subclasses (see inset). A clear correlation exists for WNL and WNE-w stars, since earlier subtypes have higher v_∞. WNE-s stars (filled circles) show generally large v_∞, but do not follow the general trend.

5.3. Terminal velocity

The terminal velocities given in Column 8 have been measured in Paper I directly from the widths of the helium lines. Much preciser values are obtained now from the detailed line fits of our "fine analyses", in some cases correcting the previous value by a few hundred km/s. Using the new values if available, v_∞ is plotted versus spectral subtype in Fig. 3. A clear correlation exists for WNL and WNE-w stars (open symbols), as earlier subtypes have higher v_∞ than later types, but the relation shows a large scatter. WNE-s stars (filled circles) show generally large terminal wind velocities and do not follow the general trend with subtype.

5.4. Radius, luminosity and mass

Any WR model which reproduces the line spectrum can be scaled in order to match a given absolute magnitude M_v by means of the "transformation law" (Eq. 1, cf. also Paper I). Keeping T_*, R_t and v_∞ fixed, this yields the parameters R_* and $\dot{M}$ in absolute units. In the course of the "fine analyses" presented here we adjusted the model parameters iteratively not only for the line fit, but simultaneously in order to meet the "observed" absolute magnitude without any final scaling being necessary.

The obtained stellar radii R_* and luminosities L are given in Columns 9 and 11, respectively. The latter is related to T_* and R_* via the Stefan-Boltzmann law From the stellar temperatures T_* and luminosities L an empirical Hertzsprung-Russell diagram (HRD) can be constructed now (Fig. 4). As in the previous figures, the WNL, WNE-w and WNE-s stars are distinguished by triangles, squares or circles, respectively. Filled symbols represent stars with hydrogen in their atmospheres, while open symbols indicate that hydrogen is not detectable.

Most WN stars are concentrated in a small, almost vertical strip of the HRD, located between 30 kK and 40 kK. The more luminous part is populated by the WNL subclass ($10^{5.3}$ ... $10^{5.9}\,L_\odot$), while the WNE-w subclass forms the continuation of that strip towards smaller luminosities down to $10^{4.6}\,L_\odot$, stressing the close relationship between the WNL and the WNE-w subclass. The WNE-s stars form a separate group of higher temperature and intermediate luminosities. The special role of the WN2-w and WN3-w stars is obvious from their stellar temperatures; note that the luminosities of WR 3 and WR 46 only rely on the M_v calibration.

The WNL stars of highest luminosities are all "hydrogen-positive". At intermediate and small L evidently only the coolest stars show hydrogen, while the "hotter" WNL, WNE-w and all WNE-s stars are hydrogen-free. The outstanding exceptions already identified in the log T_*-log R_t-plane (Fig. 2) are again WR 136 and WR 152.

The last column in Table 3 gives the stellar mass, derived from the luminosity by means of the mass-luminosity relation for helium stars (Langer 1989). Note that this relation might not be adequate for those stars showing hydrogen.

Table 3. Parameters of the Galactic single WN stars

WR	Type	d?	T_*	$T_{2/3}$	R_t	$R_{2/3}$	v_∞	R_*	$\log \dot{M}$	$\log L$	β_H	$\frac{\dot{M} v_\infty}{L/c}$	M
			[kK]	[kK]	[$R_\odot$]	[R_*]	[km/s]	[$R_\odot$]	[$M_\odot$/yr]	[$L_\odot$]	[%]		[$M_\odot$]
(1)	(2)	(3)	(4)	(5)	(6)	(7)	(8)	(9)	(10)	(11)	(12)	(13)	(14)
1	WN5-s	:	70	40	2.6	3.0	2000	2.2	-4.2	5.0	0	59.8	9.1
2^N	WN2-w	:	?	?	?	?	3100	?	?	?	0	?	?
3^N	WN3a-w +c		85	83	17.7	1.04	2500	2.4	-5.3	5.4	0	2.3	15.3
6	WN5-s +c?	+	71	41	2.6	3.0	1700	2.7	-4.1	5.2	0	36.8	11.8
7	WN4-s		90	50	2.6	3.3	1600	1.5	-4.6	5.1	0	17.1	10.3
10*	WN4.5-w	:	35.5	35.0	27.3	1.03	1500	7.2	-5.1	4.9	25	8.1	7.9
12*	WN7 +c	?	32.2	27.7	14.7	1.35	1100	16.0	-4.3	5.4	27	11.1	14.6
16	WN8		30.6	30.0	17.0	1.04	900	25.7	-4.2	5.7	[b]20	5.7	22.1
18	WN5-s	?	90	50	2.5	3.3	2100	1.6	-4.4	5.2	0	30.9	10.9
20*	WN4.5-w		36.3	33.6	12.7	1.17	1400	6.1	-4.7	4.8	0	22.3	7.0
22	WN7a +c	+	31.6	31.6	31.6	1.00	1000	30.2	-4.4	5.9	[d]40	2.3	28.9
24	WN7a	+	33.1	33.1	35.5	1.00	1200	25.7	-4.5	5.8	[b]44	2.5	26.6
25	WN7a	+	34.4	34.4	37.6	1.00	1200	18.8	-4.8	5.6	[b]53	2.3	20.3
28	WN7				— no observation —								
29	WN7				— no observation —								
34	WN4.5-w		37.2	34.8	12.0	1.14	1200	6.0	-4.8	4.8	0	16.3	7.2
35*[h]	WN6-w		37.5	31.4	11.7	1.43	1100	9.4	-4.5	5.2	22	11.1	11.4
36	WN4-s		59	35.5	2.6	2.8	2100	3.4	-3.9	5.1	0	107.0	10.1
37	WN3-s		60	41	3.7	2.2	2150	4.5	-3.9	5.3	0	53.7	13.8
40	WN8		31.0	29.8	12.0	1.08	1000	15.8	-4.2	5.3	[d]15	14.4	13.3
44	WN4-w		38.0	35.9	13.8	1.12	1400	5.2	-4.9	4.7	0	17.7	6.6
46^N	WN3pec-w		86	84	14.3	1.06	2300	2.4	-5.2	5.5	0	2.5	15.7
49*	WN5-w		36.5	34.1	16.3	1.15	1450	7.2	-4.8	4.9	25	14.6	8.3
51	WN4-w	+	36.3	35.1	17.4	1.07	1300	5.0	-5.1	4.6	0	13.3	5.8
54	WN4-w		41	37.7	12.3	1.17	1300	4.9	-4.9	4.8	0	4.2	7.0
55	WN7		33.9	32.2	11.8	1.11	1100	14.1	-4.2	5.4	0	13.4	14.2
58	WN4-s		80	48	3.1	2.8	1600	2.1	-4.4	5.2	0	17.1	11.9
61	WN4.5-w		35.5	33.8	13.5	1.10	1400	6.5	-4.7	4.8	0	21.7	7.0
62	WN6-s		48	35.3	4.2	1.85	1800	7.2	-3.8	5.4	0	59.6	14.6
63	WN6				— no observation —								
66*	WN8	?	32.1	30.5	14.2	1.11	1500	12.4	-4.3	5.2	5	24.5	11.1
67	WN6-w	:	35.1	33.5	13.2	1.10	1500	8.7	-4.5	5.0	0	23.3	9.2
71	WN6 +c				— no observation —						[f]0		
74*	WN7	?	32.4	28.1	13.2	1.33	1300	20.4	-4.0	5.6	0	15.7	19.3
75	WN6-s	?	62	34.3	2.1	3.3	2300	2.3	-4.0	4.9	0	161.6	7.9
78*	WN7	:	31.3	30.0	23.0	1.09	1200	26.3	-4.2	5.8	15	5.9	23.9
82*	WN8		32.4	28.3	14.2	1.31	1100	15.2	-4.3	5.4	20	11.6	14.0
83	WN6				— no observation —								
84	WN6-w		33.7	32.1	12.3	1.10	1100	10.2	-4.5	5.1	0	15.1	10.0
85	WN6				— no observation—						[f]+		
87*	WN7	+	31.3	31.0	39.1	1.02	1400	22.9	-4.6	5.7	40	3.9	20.3
89*	WN7	+	31.2	30.8	32.8	1.03	1600	30.6	-4.2	5.9	20	5.7	28.5
91*	WN6-s		37.5	27.7	7.3	1.83	1700	11.6	-3.9	5.4	0	47.1	14.4
94	WN6				— no observation —								
100	WN6-s		45	34.6	4.7	1.67	1600	9.0	-3.8	5.5	0	46.0	15.9
105*	WN8	:	29.8	27.2	16.4	1.20	700	28.7	-4.2	5.8	17	3.8	23.9
107	WN7-8				— no observation —								
108	WN9		30.9	30.7	28.2	1.01	900	26.9	-4.5	5.8	[a]27	2.5	23.9
109	WN3				— no observation —								
110	WN6-s	?	71	37.3	1.9	3.6	2300	1.8	-4.1	4.9	[c]0	128.3	7.7

(to be continued)

Table 3. (continued)

WR	Type	d?	T_*	$T_{2/3}$	R_t	$R_{2/3}$	v_∞	R_*	$\log \dot{M}$	$\log L$	β_H	$\frac{\dot{M} v_\infty}{L/c}$	M
			[kK]	[kK]	[$R_\odot$]	[R_*]	[km/s]	[$R_\odot$]	[$M_\odot$/yr]	[$L_\odot$]	[%]		[$M_\odot$]
(1)	(2)	(3)	(4)	(5)	(6)	(7)	(8)	(9)	(10)	(11)	(12)	(13)	(14)
115	WN6-w	:	33.9	32.9	16.8	1.06	1280	11.1	-4.6	5.2	0	12.0	11.0
116*	WN8		31.7	26.1	9.0	1.48	800	15.2	-4.2	5.3	10	13.4	13.3
120	WN7	?	33.0	31.8	13.3	1.08	1020	14.6	-4.3	5.4	0	10.5	13.9
123*	WN8 +c		31.6	29.9	13.3	1.12	1020	16.0	-4.3	5.4	0	11.8	14.0
124	[WN8]? +c		30.2	29.3	13.2	1.06	700	16.6	-4.4	5.3	[b]13	6.7	13.2
128	WN4-w +c		35.5	34.8	21.9	1.04	1500	5.8	-5.1	4.7	[d]20	12.8	6.3
129	WN4-w		35.9	34.2	14.1	1.10	1320	5.4	-4.9	4.6	0	18.9	6.0
130*	WN8		30.7	28.5	17.6	1.16	1000	26.6	-4.1	5.8	12	6.5	23.2
131*	WN7a		31.4	30.7	28.4	1.04	1400	26.4	-4.3	5.8	20	5.7	24.2
134	WN6-s +c	:	66	39.4	2.7	2.8	1900	3.0	-4.1	5.2	0	55.3	11.1
136[i]	WN6-s +c	:	53	38.5	4.5	1.90	1600	5.7	-4.0	5.4	[e]12	34.4	14.0
138	WN6a-w +c	:	33.3	32.8	22.6	1.03	1500	13.6	-4.6	5.3	[c]5	10.2	13.1
141	WN6-w +c	+	36.5	34.3	12.2	1.13	1720	9.7	-4.3	5.2	0	28.1	11.1
147*	WN7 +c[g]		31.5	29.3	13.8	1.15	1000	16.0	-4.3	5.4	5	11.0	13.8
148*	WN7 +c		31.2	30.6	26.7	1.04	1000	26.6	-4.4	5.8	15	3.3	24.2
149*	WN6-s		42	30.3	7.8	1.93	1100	12.3	-4.1	5.6	0	11.1	19.8
152*	WN3-w	:	49	47	15.2	1.10	1800	3.0	-5.2	4.7	16	12.0	6.3
155*	WN7 +c	:	32.5	32.2	28.6	1.02	1300	21.5	-4.5	5.7	0	4.8	20.6
156*	WN8		30.2	27.1	18.3	1.24	700	27.0	-4.3	5.7	30	3.1	22.9
157*	WN4.5-w	+	33.9	31.3	19.2	1.17	1500	18.4	-4.3	5.6	15	10.4	19.0
158*	WN7		30.7	29.3	25.1	1.10	900	26.8	-4.4	5.8	30	3.1	23.5

Column 3: distance known from definite ("+"), probable (":"), or possible ("?") open cluster or association membership
* Parameters obtained from a "fine analysis" with helium-hydrogen models (this paper)
N Parameters obtained from a "fine analysis" including nitrogen (Wessolowski et al., in preparation); results for WR 2 are not yet available
[a] Hydrogen mass fraction determined by Crowther et al. (1994a)
[b] Hydrogen mass fraction determined by Crowther et al. (1994b)
[c] Hydrogen mass fraction determined by Crowther et al. (in preparation)
[d] Hydrogen mass fraction determined by Hamann et al. (1991)
[e] Hydrogen mass fraction determined by Hamann et al. (1994)
[f] Hydrogen presence/absence assessed by Conti et al. (1983)
[g] WR 147: binary radio source (Churchwell et al. 1992)
[h] In Paper I the absolute parameters (R_*, $\dot{M}$, L, M) of WR 35 were erroneously scaled to a wrong absolute brightness
[i] In Paper I the absolute parameters (R_*, $\dot{M}$, L, M) of WR 136 were scaled to a wrong absolute brightness (cf. Table 2)

5.5. Mass-loss rate and momentum ratio

The mass-loss rates of the Galactic WN stars are given in Column 10 of Table 3, and plotted in Fig. 5 versus luminosity. The hydrogen-free WN stars (open symbols) nicely follow the tentative fit relation

$$\log(\dot{M}/(M_\odot\ \mathrm{yr}^{-1})) = 1.5 \log(L/L_\odot) - 11.95 \qquad (2)$$

indicated by the dashed line. Interestingly, for OB stars a relation with the same slope is established empirically and understood theoretically in terms of the theory for radiation-driven stellar winds (indicated at the lower-right corner of Fig. 5). The proportionality factor is about 100 times smaller for OB stars than for the hydrogen-free WN stars. Those WN stars showing hydrogen are found to have systematically lower mass-loss rates than the hydrogen-free WN-stars, bridging the gap to the OB star values. We will investigate this correlation quantitatively in Sect. 5.6.

The WNE-w stars of earliest subtypes WR 3 and WR 46 have exceptionally low mass-loss rates for their luminosity, compared with the fit relation for the hydrogen-free WN stars. The mass-loss rates of WC stars, on the other hand, are generally higher, as suggested by five stars (diamonds in Fig. 5) of subtypes WC5 and WC6 with known distance analyzed by Koesterke & Hamann (1994).

The ratio between the mechanical momentum carried with the wind and the momentum of the radiation field, $\dot{M} v_\infty c/L$, is given in Column 13 of Table 3. These numbers largely exceed the "single-scattering limit", i.e. unity, the arithmetic averages being 8, 14 and 58 for the WNL, WNE-w and WNE-s subclass,

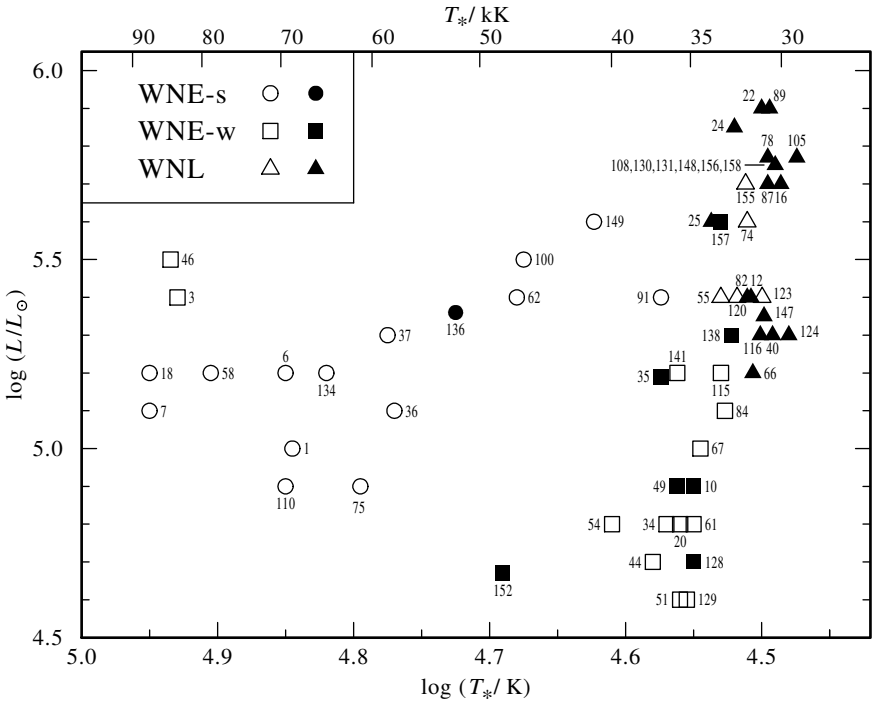

Fig. 4. Hertzsprung-Russell diagram of the Galactic WN stars (labels: WR numbers). Different symbol shapes refer to the spectral subclasses (see inset). Full symbols represent stars with hydrogen in their atmosphere, while open symbols indicate that hydrogen is not detectable. Most WN stars concentrate in an almost vertical strip at ≈ 35 kK. Its more luminous part is populated by the WNL stars, while the WNE-w subclass appears as a continuation towards lower luminosities. The WNE-w stars of earliest subtypes (WN 2 and WN 3: WR 3, 46, 152) and all WNE-s stars are considerably hotter. Hydrogen is shown by the WNL and part of the WNE-w stars, with a few exceptions.

respectively. Note, however, that WNE-s stars have "extended" atmospheres becoming optically thick at about 3 R_*, typically (cf. Table 2, Column 7). This implies that about 2/3 of the acceleration (the precise value depending on the adopted velocity law) is achieved before the continuum becomes transparent, i.e. below the photosphere! Taking only that fraction of the wind momentum produced in the optically thin part (i.e. dividing it by $R_{2/3}/R_*$), the momentum ratio for the WNE-s subclass becomes only about 20 on the average.

5.6. The hydrogen abundance

The hydrogen mass fractions determined by our detailed analyses are compiled in Table 3, Column 8. Our results are augmented from other sources (cf. table footnotes) which used the same technique of detailed modeling as the present paper.

The presence of hydrogen was estimated in Paper I only qualitatively from the H I-Balmer/He II-Pickering decrement. The detailed analyses presented now generally confirm these previous assessments, with only a few exceptions. For WR 128 (WN8 +c) the presence of hydrogen was rated as "0:" (i.e. no hydrogen detectable; the colon denotes that this result was somewhat uncertain) by Conti et al. (1983), but as "+" (i.e. hydrogen present) in our Paper I. Now we find that hydrogen is not detectable, thus confirming the former conclusion by Conti et al. (1983). For WR 91 (WN6-s) Paper I gave "+:", i.e. uncertain detection of hydrogen, while we now find "0" hydrogen being appropriate. Vice versa, in WR 148 (WN7 +c) hydrogen was not detected ("0") by Conti et al. (1983) and by Paper I (giving "0:"), while now a hydrogen mass fraction of 15% is obtained. In other cases (WR 20, 105, 138) uncertain results (with ":") from Paper I are confirmed now. For the six WN stars newly analyzed here the hydrogen presence was not studied before.

Including these new data and accounting for the mentioned corrections, the presence or absence of hydrogen was already encoded in the above Figs. 2, 4 and 5 by filled and open symbols, respectively.

Looking now for quantitative correlations with other parameters, an interesting pattern is discovered when plotting $\beta_{\rm H}$ versus the stellar luminosities (Fig. 6). All WN stars are definitely hydrogen-deficient, compared to the solar value. 53% of the Galactic WN stars (33 out of 62) are hydrogen-free, populating a luminosity range from $10^{4.6}$ to $10^{5.7}\,L_\odot$. Only three WN stars are found with hydrogen mass fractions as small as ≈ 5%, although this is well above the detection limit. Most WN stars showing hydrogen exhibit mass fractions $\beta_{\rm H}$ between 10% and 30%. They cover the whole luminosity range of the hydrogen-free WN stars, but extend also to higher values: a group of ten WNL stars with hydrogen is brighter than $10^{5.7}\,L_\odot$, i.e. brighter than any hydrogen-free WN star. A small group of four WN7 stars with high luminosities ($> 10^{5.6}\,L_\odot$) has outstandingly high hydrogen mass fractions (40 ... 53%).

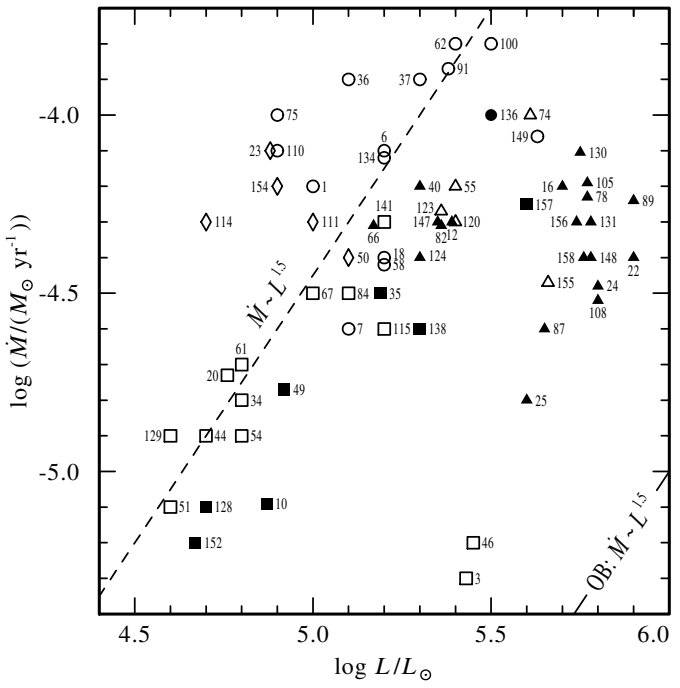

Fig. 5. Mass-loss rates of Galactic WR stars versus luminosity. The individual stars are labeled by their WR number. Triangles, squares and circled refer to WNL, WNE-w and WNE-s stars, respectively. Five WC stars with well-established data (Koesterke & Hamann 1994) are also represented (diamonds). Filled and open symbols indicate whether hydrogen is detectable or absent, respectively. The dashed line gives a tentative fit to the mass-loss rates of hydrogen-free WN stars (Eq. 2), while those WN stars with hydrogen lie to the lower-right of that relation. The corresponding relation for OB stars is indicated at the lower-right corner.

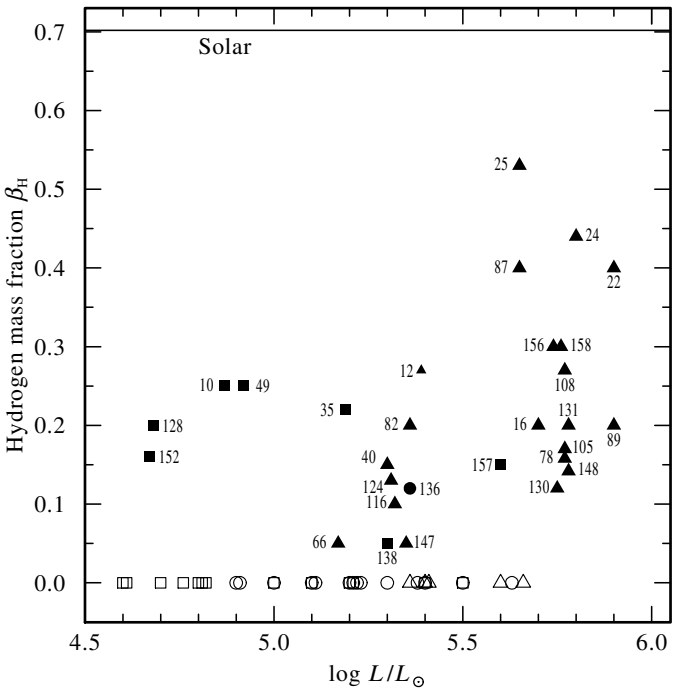

Fig. 6. Hydrogen abundances in the Galactic WN stars versus stellar luminosities. The filled symbols are identified by the corresponding WR number, while the symbol shape indicates the spectral subtype as in the previous figures. Stars showing no hydrogen (open symbols) are crowding at the zero level.

We propose to discuss the stellar evolution by means of the hydrogen-versus-luminosity diagram (Fig. 6). The standard calculations producing Wolf-Rayet stars by "post red supergiant" evolution fail to explain the observed luminosities and hydrogen abundances. Langer et al. (1994 – see there for more details on this subject) proposed a new scenario relating O stars, Luminous Blue Variables (LBVs) and Wolf-Rayet stars by accounting for pulsation-driven mass-loss. According to their pilot calculation, a star starting with $60 M_\odot$ at the Main Sequence evolves to a hydrogen-rich WNL star (corresponding to the group formed by WR 22, 24, 25 and 87) without becoming a red supergiant before. After strong mass ejection in the LBV phase a second WN phase with smaller hydrogen abundance follows, and the hydrogen-free layers finally appear at the surface while the luminosity decreases significantly.

In Fig. 5 we have seen that the mass-loss rates of hydrogen-free WN stars follow a relation $\dot{M} \propto L^{1.5}$, while WN stars with hydrogen are bridging the gap to the OB stars which have 100 times smaller $\dot{M}$, but with the same luminosity dependence. Indeed, those four WN7 stars with the highest hydrogen mass fraction (WR 22, 24, 25, 87) are found to lie closest to the OB relation.

This is illustrated quantitatively in Fig. 7 by plotting β_H versus $\log \dot{M} - \log L^{1.5}$. Thus a constant x-value of -11.95 would correspond to the fit relation for hydrogen-free WN stars (cf. Fig. 5 and Eq. 2), as reflected by the crowding of the open symbols around this point. Only three open symbols are lying apart, namely the WN3-w stars WR 3 and 46 which differ in many aspects from the other spectral subgroups, and the WNL star WR 155 which is peculiar in showing no hydrogen (cf. Figs. 2 and 4). The typical OB-star relation is represented by the asterisk at solar hydrogen abundance (although many OB stars are actually more or less helium-enriched, cf. Herrero et al. 1992). Fig. 7 reveals that the WN stars follow nicely the shaded interpolation line, i.e. the gradual switching between the mass-loss laws for OB stars and for hydrogen-free WN stars is correlated with the hydrogen/helium abundance. This might perhaps simply reflect that both, helium abundance and mass-loss rate, increase during the course of the evolution due to the changes of the stellar structure and parameters. But this correlation might even indicate that the mechanism which defines the mass-loss rate (pulsational instability?) is damped by the presence of hydrogen in the outer layers, leaving only the radiation-driven wind in the case of solar composition.

A similar, but less well-defined correlation as in Fig. 7 would be obtained when plotting the hydrogen mass fraction versus the momentum ratio $\dot{M} v_\infty c/L$ (cf. Column 13 of Table 3). Thus it seems that it is the initializing of the stellar wind rather

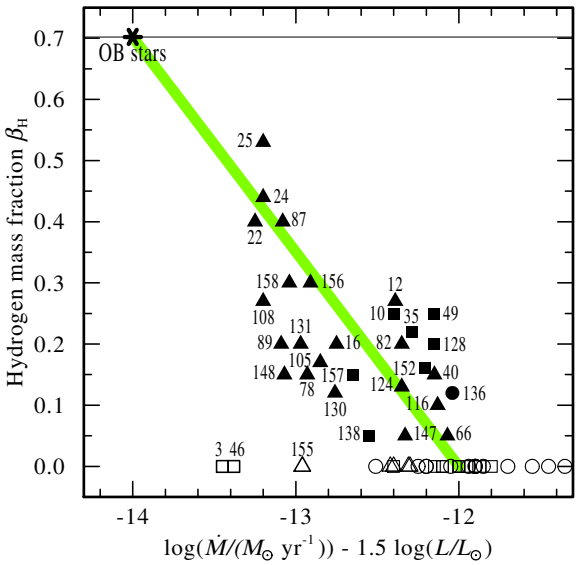

Fig. 7. Hydrogen mass fraction β_H versus $\log \dot{M} - \log L^{1.5}$. Thus a constant x-value of -11.95 would correspond to the fit relation for hydrogen-free WN stars (cf. Fig. 5 and Eq. 2), as reflected by the crowding of the open symbols around this point. The typical OB-star relation is represented by the asterisk at solar hydrogen abundance. The WN stars follow nicely the shaded interpolation line, i.e. the gradual switching between the mass-loss laws for OB stars and for hydrogen-free WN stars is correlated with the hydrogen/helium abundance.

than the final acceleration which is correlated to the chemical composition.

6. Conclusion

The fundamental stellar and atmospheric parameters, including the hydrogen/helium abundances, are available now for almost all Galactic WN stars. These data provide a broad empirical basis for discussing their evolutionary status and the mass-loss mechanism.

Acknowledgements. L.K. acknowledges support from the Deutsche Forschungsgemeinschaft under grant Ha 1455/4-2, and U.W. from the Bundesministerium für Forschung und Technologie under grant 50 OR 9302 4.

References

Castor J.I., Van Blerkom D., 1970, ApJ 161, 485
Churchwell E., Bieging J.H., van der Hucht K.A., Williams P.M., Spoelstra T.A., Abbott D.C., 1992, ApJ 393, 329
Crowther P.A., 1993, PhD Thesis, University College London
Crowther P.A., Hillier D.J., Smith L.J., 1994a, A&A (in press)
Crowther P.A., Hillier D.J., Smith L.J., 1994b, A&A (submitted)
Conti P.S., Leep E.M., Perry D.N., 1983, ApJ 268, 228
Garmany C.D., Conti P.S., 1984, ApJ 284, 705
Hamann W.-R., 1985, A&A 148, 364
Hamann W.-R., 1986, A&A 160, 347
Hamann W.-R., 1987, in: Numerical Radiative Transfer, ed. W. Kalkofen, Cambridge University Press, p. 35
Hamann W.-R., 1994, Space Science Reviews 66, 237
Hamann W.-R., Schmutz W., 1987, A&A 160, 347
Hamann W.-R., Wessolowski U., 1990, A&A 227, 171
Hamann W.-R., Schmutz W., Wessolowski U., 1988, A&A 194, 190
Hamann W.-R., Dünnebeil G., Koesterke L., Schmutz W., Wessolowski U., 1991, A&A 249, 443
Hamann W.-R., Leuenhagen U., Koesterke L., Wessolowski U., 1992, A&A 255, 200
Hamann W.-R., Koesterke L., Wessolowski U., 1993, A&A 274, 397 (Paper I)
Hamann W.-R., Wessolowski U., Koesterke L., 1994, A&A 281, 184
Herrero A., Kudritzki R.P., Vilchez J.M., Kunze D., Butler K., Haser S., 1992, A&A 261, 209
Hillier D.J., 1990, A&A 231, 116
Howarth I.D., Schmutz W., 1992, A&A 261, 503
van der Hucht K.A., Conti P.S., Lundström I., Stenholm B., 1981, Space Sci. Rev. 28, 227
van der Hucht K.A., Hidayat B., Admiranto A.G., Supelli K.R., Doom C., 1988, A&A 199, 217
van der Hucht K.A., 1992, A&AR 4,123
Koesterke L., Hamann W.-R., 1994, A&A (submitted)
Koesterke L., Hamann W.-R., Schmutz W., Wessolowski U., 1991, A&A 248, 166
Koesterke L., Hamann W.-R., Kosmol P., 1992, A&A 255, 490
Kuhi L.V., 1968, in "Wolf-Rayet Stars", K.B. Gebbie, R.N. Thomas (eds.), NBS SP-307, p. 101
Langer N., 1989, A&A 210, 93
Langer N., Hamann W,-R., Lennon M., Najarro F., Pauldrach A.W.A., Puls J., 1994, A&A (in press)
Leung K.-C., Moffat A., Seggewiss W., 1983, ApJ 265, 961
Lundström I., Stenholm B., 1984, A&AS 58, 163
Schmutz W., Hamann W.-R., Wessolowski U., 1988, in "Atmospheric Diagnostics of Stellar Evolution: Chemical Peculiarity, Mass Loss and Explosion", Proceedings of the 108th IAU Colloquium, Tokyo 1987, p. 143
Schmutz W., Hamann W.-R., Wessolowski U., 1989, A&A 210, 236
Smith L.F., 1968, MNRAS 140, 409
Smith L.F., 1973, in "Wolf-Rayet and High Temperature Stars", IAU Symp. 49, M.K.V. Bappu and J. Sahade (eds.), Reidel, Dordrecht, p. 15
Springmann U., 1994, A&A 289, 505
Vreux J.-M., Andrillat Y., Biemont E., 1990, A&A 238, 207
Wessolowski U., Schmutz W., Hamann W.-R., 1988, A&A 194, 160
Wilson O.C., 1940, PASP 52, 404

This article was processed by the author using Springer-Verlag LaTeX A&A style file *L-AA* version 3.